

Mastering disorder in a first-order transition by ion irradiation

S. Cervera,¹ M. LoBue,² E. Fontana,^{1,3,*} M. Eddrief,¹ V.H. Etgens,^{1,†} E. Lamour,¹ S. Macé,¹ M. Marangolo,¹ E. Plouet,¹ C. Prigent,¹ S. Steydli,¹ D. Vernhet,¹ and M. Trassinelli^{1,‡}

¹*Institut des NanoSciences de Paris, CNRS, Sorbonne Université, F-75005 Paris, France*

²*SATIE, ENS Paris Saclay, CNRS, Université Paris-Saclay, F-91190 Gif-sur-Yvette, France*

³*Department of Applied Science and Technology, Politecnico di Torino, I-10129 Torino, Italy*
(Dated: July 27, 2023)

The effect of ion bombardment on MnAs single crystalline thin films is studied. The role of elastic collisions between ions and atoms of the material is singled-out as the main process responsible for modifying the properties of the material. Thermal hysteresis suppression, and the loss of sharpness of the magneto-structural phase transition are studied as a function of different irradiation conditions. While the latter is shown to be associated with the ion induced disorder at the scale of the transition correlation length, the former is related to the coupling between disorder and the large-scale elastic field associated with the phase coexistence pattern.

The role of quenched disorder on phase changes has been addressed theoretically for several decades [1–5]. In the case of first-order transitions, unraveling the leading physical mechanisms responsible for the coupling between random impurities and order parameters is even a harder task. The coexistence of very different characteristic lengths and the presence of non-equilibrium features like hysteresis and kinetics make even further the task complex. Nonetheless, as most of the known large caloric effects take place on the verge of a first-order ferroic transition [6], mastering hysteresis preserving other features (i.e. entropy and temperature changes) has been the focus of many investigations for the last two decades. At stake, beside the fundamental interest, such investigations can have a direct impact on the use of caloric effects for refrigeration and energy conversion applications [7–9]. Hysteresis reduction in magnetocaloric materials has been successfully achieved acting on the phase transition globally, getting closer to a critical point through chemical change (i.e. tuning stoichiometry) [10, 11], or using a secondary external field coupled to the order parameter (e.g. hydro-static pressure, substrate strain)[12–14]. Another approach to reduce hysteresis relies on modifying the phase change mechanism using local non-homogeneity (e.g. porosity, inclusions) fostering phase nucleation. Indeed, controlling first-order phase changes in caloric materials using defects and disorder has been studied at different scales, from the atomic/chemical [15, 16], to the structural one [17, 18]. Thence, the possibility to tune the amount of disorder in a model-system represents a unique opportunity for experimental investigations on phase change in solid-state systems. Moreover, it can pave the way to develop new methods for tailoring the functional properties of materials where phase changes take place.

In this letter, we study the modifications induced by the collision and implantation of ions in manganese arsenide thin monocrystals. Bulk manganese arsenide (MnAs) shows a first-order magneto-structural transition from ferromagnetic to paramagnetic order accompanied

by a lattice symmetry switch when getting above the transition temperature $T_t = 313$ K [19]. From this perspective, MnAs can be considered as a prototypical first-order magnetocaloric material. Previous studies [20, 21] proved thermal hysteresis suppression in ion bombarded MnAs single crystal films, keeping the caloric effect intensity unchanged. Here, the mechanisms underlying the modifications of the transition after ion bombardment are investigated on single crystalline 150 nm thick MnAs films under different irradiation conditions (i.e. ion mass, ion kinetic energy, fluences, etc.).

The MnAs films have been obtained by molecular beam epitaxy on GaAs(001) 0.3 mm thick substrates. The deposited MnAs is oriented with the α -MnAs[0001] and β -MnAs[001] axis parallel to GaAs[$\bar{1}10$] [22]. In thin films, due to the epitaxial strain, the phase coexistence between the ferromagnetic α -phase with hexagonal structure (NiAs-type) and the paramagnetic β -phase with orthorhombic structure (MnP-type), takes place over an extended temperature range (280–320 K) [23], in contrast with the sharper transition observed at the temperature $T_t = 313$ K in bulk single crystals [24].

Ion irradiations have been performed at two facilities: the electron-cyclotron ion source SIMPA facility (Paris, France) [25], and the line IRRSUD facility at the GANIL accelerator (Caen, France). At SIMPA, samples have been irradiated with different ions (i.e. helium, oxygen, neon, argon and krypton) with kinetic energies ranging from 22 to 260 keV. The ion fluence Φ has been varied between 1×10^{12} ions/cm² and 6×10^{15} ions/cm², corresponding to an irradiation time spanning from few tens of seconds to several hours. The energy of the different ion beams and the incident angle have been chosen in order to reach an average penetration depth corresponding to the half thickness of the film. At IRRSUD, a beam of isotopic ³⁶Ar with an energy of 35.28 MeV has been used. In this case no ions are implanted in the MnAs film, most of them being stopped in the GaAs substrate. The fluence has been varied from 4×10^{12} to 1×10^{15} ions/cm².

During the interaction with a solid, the ion transfers

its kinetic and potential energies to the target atoms by a series of processes that can be schematically separated in two categories: one due to the interaction with the target nuclei, the other due to the interaction with the electrons. The electron interaction is inelastic, and entails small or no lattice distortion into the target. The ion energy losses, including those related to the potential energy of the ion, are transferred to the solid via excitation of phonons, with an increasing of the temperature along the trajectory. Nuclear collisions are the most probable process at low velocity and/or for heavy ions. Each collision can be assumed to be binary, and elastic [26–28]. It can lead to the displacement of sample atoms from their site, with the creation of vacancies and interstitial atoms in the sample lattice. If the energy transferred to the recoil atom is higher than twice the displacement energy of a single atom, a cascade of secondary collisions is generated, producing a cluster of defects [26]. For a same kinetic energy, heavy ions produces a higher number of collisions per ion than light ions. This is due to the higher cross-section of the primary impact, and to the more favorable momentum transfer to target atoms, as well as to the consequent secondary collisions in the cascade.

At the ion kinetic energies of SIMPA (E_{kin} less than 300 keV), the nucleus–nucleus interaction between incoming ions and sample atoms is the main process responsible for induced modifications. At the ion kinetic energies of IRRSUD, the probability of nuclear processes decreases while inelastic processes start to occur. Due to the small ion potential energy ($E_p \lesssim 5$ keV), compared to the kinetic energy, and to the metallic nature of the MnAs samples, the local heating from the electron interaction is not expected to induce noticeable modifications in the material. As we will see, elastic nuclear collisions remain the leading process that modify the properties of the irradiated sample.

The two main modifications observed after ion bombardment are hysteresis reduction, and the loss of sharpness of the transition (see Fig.1), often referred to as *rounding* [2]. To investigate them, isofield thermomagnetic $M(T)$ curves have been measured at constant field ($H = 1$ T) by a SQUID device. All the magnetization measurements have been carried along the easy magnetization direction (i.e. in the film plane, and along the easy axis). This makes the proportionality between $M(T)$ and the ferromagnetic α -phase a reliable assumption even under the application of a relatively small field of 1 T. Before each measurement, the material has been heated up to 350 K in order to erase any trace of the low-temperature phase, resetting sample history [29]. Hysteresis, transition temperatures, and rounding are extracted from $M(T)$ curves and their derivatives. Whereas hysteresis, and its reduction, are phenomena taking place close to transition temperature T_t , the transition rounding is associated with a widening of the phase coexistence region

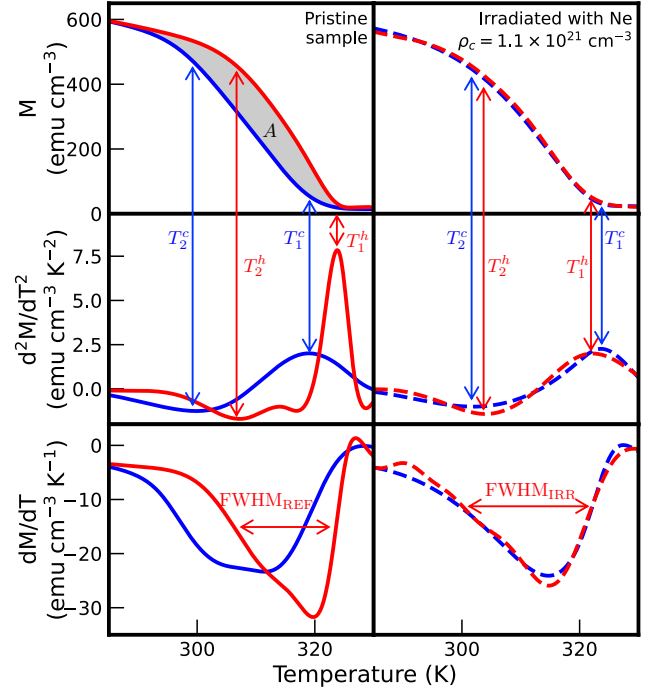


FIG. 1. Isofield ($H = 1$ T) magnetization curves $M(T)$ (top) and corresponding first (bottom) and second derivative (middle) measured on reference (left) and irradiated (right) samples. The relevant temperatures corresponding to maxima and minima of the second derivative are indicated together with the loop area A of $M(T)$ and the FWHM of the first derivative. Cooling and heating curves are represented in blue and red, respectively.

far away from it. Here, the thermal hysteresis width, ΔT_{hyst} , is evaluated from the area A between the $M(T)$ heating and cooling curves (Fig. 1 top) normalized to the saturation magnetization M_s , $\Delta T_{\text{hyst}} = A/M_s$ ¹. M_s is the magnetization measured at 100 K under the application of a field $H = 1$ T. Indeed, most samples have been irradiated within regimes where the maximum magnetization M_s is not, or is marginally modified.

Concerning the evaluation of the rounding, the data analysis has to disentangle the effect due to defects induced quenched-in disorder [13, 32] from the strain-induced broadening at the magnetostructural phase transition. The latter is characterized by a linear evolution of the phase fraction, across the transition, as a function of T . As shown in [22, 33–37], this behavior is driven by a mesoscopic phase-domain stripes pattern, and by its long-range elastic field. The former is relevant far from T_t and is associated with the presence of minority-phase regions whose stability is made possible by a local shift

¹ An approach commonly used in the field of loss, and hysteresis modelling; it amounts to consider the effective width of an equivalent rectangular hysteresis cycle. See [30, 31]

of T_i [2]. To tag the irradiation rounding effect only, we introduce the variable

$$\Delta T_{\text{rnd}} = \text{FWHM}_{\text{IRR}} - \text{FWHM}_{\text{REF}} \quad (1)$$

obtained by the width at half maximum (FWHM_{IRR}) of the first derivative of $M(T)$ of the irradiated films minus the contribution FWHM_{REF} of the pristine sample (see Fig. 1 bottom). Eventually, to identify the main part of the phase coexistence interval, the second derivative d^2M/dT^2 is used. The upper and lower bounds, T_1 and T_2 , of the steepest part of the transition are identified with the maximum and the minimum of d^2M/dT^2 respectively. Some typical irradiation induced modifications are presented, as an example, in Fig. 1 where the heating (T_1^h , and T_2^h) and cooling (T_1^c , and T_2^c) temperatures is marked over the $M(T)$ (top) and d^2M/dT^2 (middle) curves of the pristine and of an irradiated sample.

In order to disentangle the role of binary-collisions induced defects, from the one of ion implantation in modifying the target properties, we firstly compare samples features with respect to average collision density or implanted ion density, ρ_c , and ρ_i , respectively. These quantities are estimated using the applied ion fluences, and the output of the ion-matter interaction Monte Carlo code SRIM/TRIM [38, 39]. The two densities induced by bombarding a sample of thickness t with a fluence Φ are estimated through the following expressions: $\rho_i = f\Phi/t$, and $\rho_c = N_{\text{coll}}\Phi/t$, where f , is the fraction of ions stopped, and N_{coll} is the average number of binary collisions induced by a single ion in the film². For our specific cases, f , and N_{coll} have a range of $[0, 1]$ and $[50, 5000]$, respectively. Thus ρ_i and ρ_c differ by order of magnitude and strongly depend on the projectile ion characteristics

The hysteresis width ΔT_{hyst} is shown in Fig. 2 as a function of ρ_i (top frame) and of ρ_c (bottom frame). Whereas no correlation is apparent between ΔT_{hyst} and ρ_i , a clear trend can be appreciated when ΔT_{hyst} is plotted against ρ_c . More precisely, ΔT_{hyst} decreases as a function of ρ_c until its total suppression at $\rho_c \approx 10^{21} - 10^{22} \text{ cm}^{-3}$. It is noteworthy that the three points relative to fast Ar irradiation, where no ions get implanted into the sample, spread over the same hysteresis decreasing trend curve when plotted against ρ_c (bottom frame of Fig. 2). Data from fast, and slow ions follow the same tendency with respect to the collision density. This is one of the main findings of this letter, and it shows that, within the considered fluence interval, the relevant defects, in terms of

modification of the phase transition, are the ones produced by binary elastic collisions.

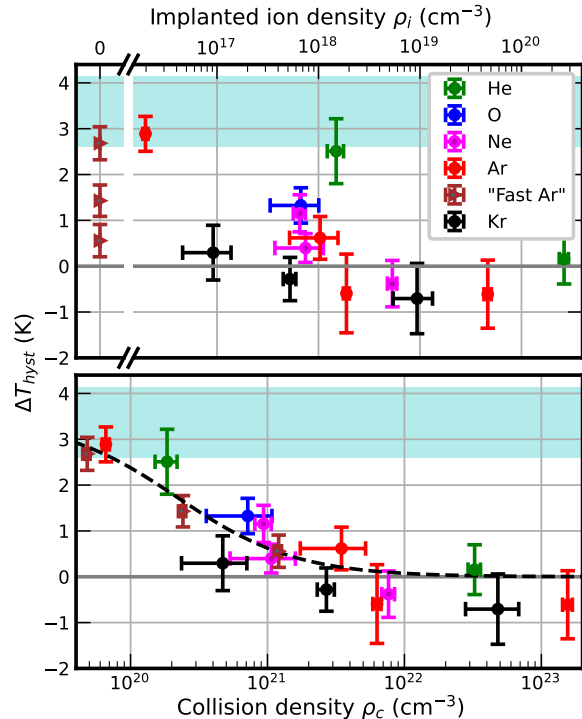


FIG. 2. Thermal hysteresis area as a function of the average density of implanted ions ρ_i (top), and of the average density of elastic collisions ρ_c (bottom). In light blue the value of the pristine sample is reported. The uncertainties on the x-axis are mainly determined by the fluence evaluation, which can be critical for some beam preparation. The uncertainty on the y-axis is due to the SQUID measurement and the interpolation of the data affected by noise. The dashed line represents the best fit of the data with the formula discussed in the text.

To get a better insight into the mechanisms underlying thermal hysteresis in MnAs films, the amplitude of the phase coexistence interval, limited by the above defined temperatures T_2 , and T_1 , is studied over heating, and cooling as a function of ρ_c . When hysteresis is present, the aforementioned second derivative maximum and minimum show different values along the cooling, and heating curves. The temperatures corresponding to these maxima, and minima are plotted in Fig. 3 as a function of the collision density ρ_c measured on heating (red), and cooling (blue).

The upper limit of the phase coexistence interval, T_1 , is unaffected by irradiation, and does not show hysteresis (i.e. values over heating and cooling are similar, they are marked with a black dashed line in Fig. 3); on the contrary, the difference $\Delta T_2 = T_2^h - T_2^c$ between T_2 over heating (T_2^h , red dashed lines and arrows), and cooling is apparent and gets reduced, and eventually suppressed, as a function of ρ_c . Following [34], T_1 can be considered as

² Despite the well-known SRIM/TRIM trend of slightly overestimating the number of induced defects [26, 28, 40], the predicted agglomerations (i.e. mixed-up vacancies and interstitials clusters) are rather similar to the ones obtained by advanced many-body molecular dynamics calculations taking into account collective behavior and temperature effects [27, 28, 41–43], and to the ones observed experimentally as well [44].

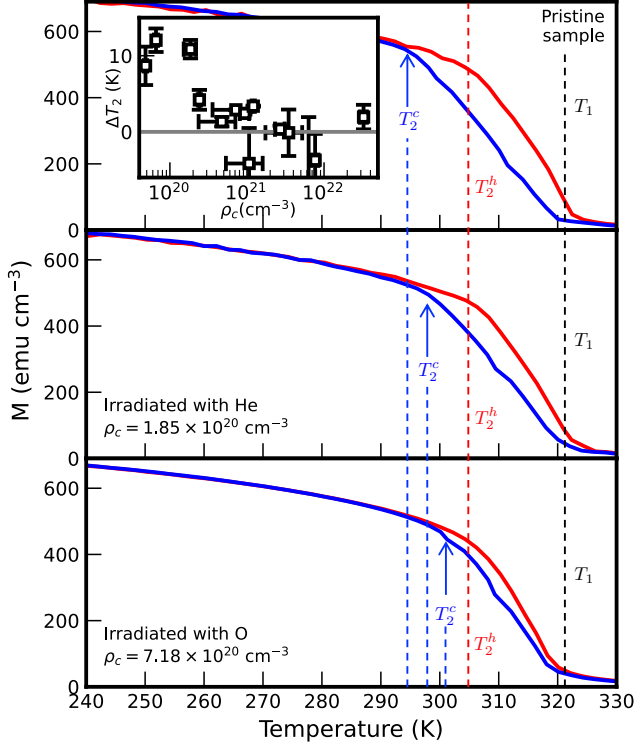


FIG. 3. Comparison between $M(T)$ loops over heating, and cooling (in red and blue), measured on the pristine sample (top), on a He irradiated sample (middle) and on an O irradiated sample (bottom). In the inset, the difference $\Delta T_2 = T_2^h - T_2^c$ between the values of T_2 over heating and cooling is shown as function of ρ_c .

the closest approximation to the actual transition point T_t (i.e. the one of a bulk single crystal). On the other hand, as apparent from Fig. 3, the reduction of hysteresis takes place as an increasing of T_2^c , in irradiated samples, with no change of T_2^h . In other words, hysteresis disappears through the collapse of the cooling $M(T)$ curve onto the heating one. Thence, hysteresis is mainly associated to supercooled metastable states.

The transition rounding ΔT_{rnd} (Eq. (1)) also shows a systematic trend as a function of the collision density ρ_c (Fig. 4, top). Its clear departure from the reference value, at $\rho_c \approx 4 \times 10^{20} \text{ cm}^{-3}$, is followed by a strong increasing with a slope depending on the ion type used for irradiation. Furthermore, the points collapse over the same curve when normalizing the relative rounding to the square root of the ion mass number m , $\Delta T_{\text{rnd}}/\sqrt{m}$ (Fig. 4, bottom).

The explanation of the observed modifications, after irradiation, is two-fold. On the one hand, rounding takes place far from T_t and is expected to be driven by the phase transition correlation length ξ ; on the other hand, hysteresis suppression takes place near T_t where stripes domains, and their long-range elastic field drive transition kinetics at the mesoscale [34]. The observed round-

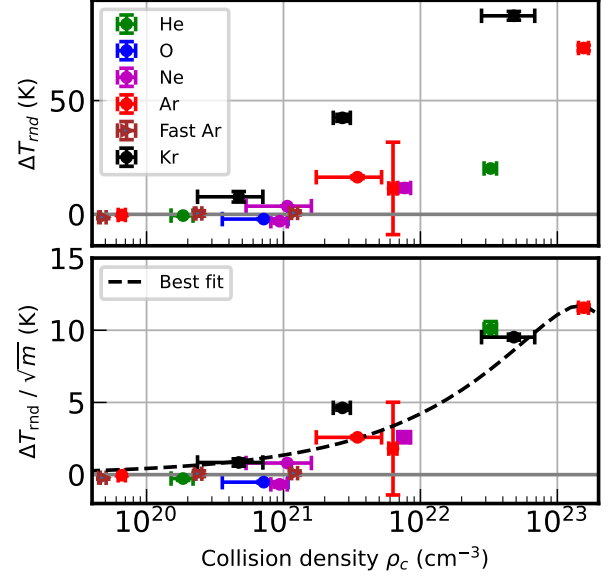


FIG. 4. Relative rounding ΔT_{rnd} from the FWHM of dM/dT curves without (top) and with \sqrt{m} mass rescaling (bottom). The dashed line represents the best fit of the data with the function $f(p) = c\sqrt{p(1-p)}$ (see text).

ing behavior fits pretty well within the approach reported in [2]. Considering a magnetic lattice model with a probability p to get a lattice site occupied by some sort of impurity, it is shown that, even when $p \ll 1$, a relevant transition rounding can appear due to the local fluctuations of impurity density. For a random impurity distribution, density fluctuations are proportional to the variance $p(1-p)$. The key issue to get a stable rounding is the relationship between the phase transition correlation length ξ , and the characteristic size L of the regions where the impurity density fluctuation makes the minority phase (i.e. the high temperature phase when $T < T_t$, or the low temperature one when $T > T_t$) energetically favored. Thence, the smearing-out of the transition is driven by the dimensionality d of the magnetic system, and by the way the interface energy between the two phases scales with respect to the region size L . Following [2], a spin lattice of dimensionality $d = 3$, with discrete symmetry, and with a surface tension between phases over a region of size L scaling as L^2 is expected to be unaffected by quenched disorder when $L < \xi$. Rounding appears when $L \sim \xi$, and scales as $\sqrt{p(1-p)}/L^3$ when $L > \xi$. Assuming the probability p , to get an impurity to be $p \propto \rho_c$, from Fig. 4 it can be deduced that $\xi \sim L$ when $\rho_c \approx 4 \times 10^{20} \text{ cm}^{-3}$. From cascade simulations, the typical volume of collision clusters is known to be $\propto 1/m$, where m is the ion mass. Assuming elastic-collision cascades as the origin of the impurities implies $L^3 \propto 1/m$, a feature that explains the higher slopes showed by samples irradiated with heav-

ier ions, and the collapse of all the points onto the same curve after the $1/\sqrt{m}$ normalization³. Figure 4 (bottom) shows the mass normalized relative rounding data fitted with a function $f(\rho_c) = c\sqrt{a\frac{\rho_c}{\rho_0}\left(1 - a\frac{\rho_c}{\rho_0}\right)} \equiv c\sqrt{p(1-p)}$.

$\rho_0 = 2.92 \times 10^{22} \text{ cm}^{-3}$ is the atomic density of MnAs and a is a proportionality constant between p and ρ_c/ρ_0 that incorporates possible auto-healing processes, not taken into account by SRIM/TRIM, and possible activation thresholds. A value of $a = (9.7 \pm 0.6)\%$ is found.

This shows that far away from the transition temperature, the minority phase (i.e. the β -phase at low, and the α -one at high temperature) develops as randomly distributed droplets before the building-up of the elastic-domain stripe structure. This has been observed by scanning probe microscopy [35], and by atomic force microscopy [37]. Actually, whereas closer to T_t energy minimization is dominated by the long-range elastic interaction between stripes [33], in the first stages of the transition the leading energy terms are local, and fully led by the size L of regions where the precursor develops.

Hysteresis is suppressed by ion bombardment within the collision density interval $3 \times 10^{20} \text{ cm}^{-3} \lesssim \rho_c \lesssim 10^{21} \text{ cm}^{-3}$, as apparent in Fig. 3. However, as clearly put in [34], after the first nucleation stage the phase-coexistence stripes pattern builds-up and the resulting thermal hysteresis can hardly be explained through a droplet-nucleation mechanism. Actually, while only the cooling dM/dT curve plotted in Fig. 1 (bottom) for the non-irradiated sample shows a good agreement with the linear phase-evolution picture described in Refs. [33, 34], all the other curves show a non-linear $M(T)$. Besides, Fig. 1 (bottom) shows that hysteresis reduces jointly with the loss of linearity of the cooling $M(T)$ curve. Higher values of the maximum of dM/dT implying a faster phase kinetics. Similar asymmetries of transition kinetics are a rather common feature of first order phase transitions, from the best known example of the water-ice transition to the different kinetics observed under cooling, and heating in FeRh films [45]. Here, as noticeable in Fig.3, the difference between the cooling, and heating $M(T)$ curves depends on the lower slope of the formers, and on the entailed lower T_2 (i.e. a coexistence region lasting till a lower temperature). Furthermore, the observed loss of linearity of the cooling curves, and their increasing slope, going hand-in-hand with hysteresis reduction, can be interpreted as a modification of the elastic field associated with the stripes domain structure.

A possible clue to explain this behavior comes from the observation of the distortion of the regular stripes pattern in MnAs films after ion irradiation [20], with an

an increasing density of finite-length stripes. These defects have been observed in non-irradiated samples too [22, 36, 37]. They are associated to the non-linear region of $M(T)$ and they mostly disappear within the ordered stripes structure getting closer to the transition temperature. Finite-length stripes are expected to behave as topological defects, modifying the elastic energy with their stress field, similarly to the way unbound edge-dislocations do in 3D solids [46, 47], and in 2D mesomorphic phases [48]. Their increased density in irradiated samples⁴ can be at the origin of the suppression of the supercooled metastable states underlying hysteresis, either by changing the phase fraction through nucleation of pairs or by renormalizing the effective elastic constants.

This explanation, still rather conjectural, makes the point that ion-induced disorder directly modifies the phase-domain patterning. In this case, the relevant scale is the phase-domain characteristic length (i.e. the stripes spacing, $d_s \approx 0.73 \mu\text{m}$ [20]). Over such a large scale, the average collision density $\rho_c \propto p$ is expected to be the relevant quantity. The dashed curve in Fig. 2 (bottom) is obtained using as a fitting function $f(\rho_c) \propto 1/(p_0 + a \rho_c/\rho_0)$, where p_0 is a constant describing the impurities present in the sample before the irradiation, which is found to be $p_0 = (7.3 \pm 2.3) \times 10^{-4}$. It shows that, besides reducing hysteresis, collision-induced defects can be used to tailor the film domain pattern in the phase coexistence region.

To conclude: in this letter, we address the changes induced in MnAs thin films by ion irradiation. It is shown that elastic ion-atom collisions are the main mechanism responsible for modifying the magnetic properties of the material. Besides, modifications induced by ion collisions are shown to act at two different scales. At the short range, collisions serves as nucleation seeds of precursors responsible for the loss of sharpness of the phase change far from the transition temperature. At a larger scale, collisions modify the elastic energy by softening the long-range elastic field associated with the substrate coupling. Thus new topological defects creation is favored in a distorted stripe pattern and the thermal hysteresis is reduced until its elimination.

Disorder induced by light ions irradiation of magnetic thin films has been recently investigated through domain wall motion measurements focusing on spintronics applications [49]. Here, the effect of irradiation with ions of different mass is investigated through the behavior of the first order magneto-structural transition on MnAs thin epitaxial films. Hysteresis suppression, transition rounding, and the tailoring of the phase-domain pattern are observed opening unique opportunities in terms of applications to magnetocaloric devices, and to design of novel magnetic heterostructures.

³ Similar curves can be obtained by normalizing with respect to the number of collision per ion and average size of clusters of defects.

⁴ as shown in Fig.3 of [20]

The authors acknowledge the staff (and in particular D. Hrabovsky) of the MPBT (physical properties - low temperature) platform of Sorbonne Université for their support. This work was supported by French state funds managed by the ANR within the Investissements d'Avenir programme under reference ANR-11-IDEX-0004-02, and within the framework of the Cluster of Excellence MATISSE led by Sorbonne Universités, and of the project HiPerTher-Mag (ANR-18-CE05-0019).

* Present address: Institut Néel, CNRS, F-38042, Grenoble, France

† Present address: Centre de recherche et de restauration des musées de France, F-75001 Paris

‡ martino.trassinelli@insp.jussieu.fr

- [1] A. Brooks Harris, "Effect of random defects on the critical behaviour of Ising models," *J. Phys. C: Solid State Phys.* **7**, 1671 (1974).
- [2] Yoseph Imry and Michael Wortis, "Influence of quenched impurities on first-order phase transitions," *Phys. Rev. B* **19**, 3580 (1979).
- [3] James P Sethna, Karin Dahmen, Sivan Kartha, James A Krumhansl, Bruce W Roberts, and Joel D Shore, "Hysteresis and hierarchies: Dynamics of disorder-driven first-order phase transformations," *Phys. Rev. Lett.* **70**, 3347 (1993).
- [4] A. Berger, A. Inomata, J.S. Jiang, J.E. Pearson, and SD Bader, "Experimental observation of disorder-driven hysteresis-loop criticality," *Phys. Rev. Lett.* **85**, 4176 (2000).
- [5] T.R. Kirkpatrick and D. Belitz, "Stable phase separation and heterogeneity away from the coexistence curve," *Phys. Rev. B* **93**, 144203 (2016).
- [6] X. Moya, S. Kar-Narayan, and N. D. Mathur, "Caloric materials near ferroic phase transitions," *Nat. Mater.* **13**, 439–450 (2014).
- [7] O. Gutfleisch, T. Gottschall, M. Fries, D. Benke, I. Radulov, K. P. Skokov, H. Wende, M. Gruner, M. Acet, P. Entel, and M. Farle, "Mastering hysteresis in magnetocaloric materials," *Phil. Trans. R. Soc. A* **374**, 20150308 (2016).
- [8] Julia Lyubina, "Magnetocaloric materials for energy efficient cooling," *J. Phys. D* **50**, 053002 (2017).
- [9] Tino Gottschall, Konstantin P. Skokov, Maximilian Fries, Andreas Taubel, Iliya Radulov, Franziska Scheibel, Dimitri Benke, Stefan Riegg, and Oliver Gutfleisch, "Making a cool choice: The materials library of magnetic refrigeration," *Adv. Energy Mater.* **9**, 1901322 (2019).
- [10] E. Brück, N.T. Trung, Z.Q. Ou, and K.H.J. Buschow, "Enhanced magnetocaloric effects and tunable thermal hysteresis in transition metal pnictides," *Scr. Mater.* **67**, 590–593 (2012).
- [11] V. Franco, J. S. Blázquez, J. J. Ipus, J. Y. Law, L. M. Moreno-Ramírez, and A. Conde, "Magnetocaloric effect: From materials research to refrigeration devices," *Prog. Mater. Sci.* **93**, 112–232 (2018).
- [12] Jian Liu, Tino Gottschall, Konstantin P. Skokov, James D. Moore, and Oliver Gutfleisch, "Giant magnetocaloric effect driven by structural transitions," *Nat. Mater.* **11**, 620–626 (2012).
- [13] D. H. Mosca, F. Vidal, and V. H. Etgens, "Strain engineering of the magnetocaloric effect in MnAs epilayers," *Phys. Rev. Lett.* **101**, 125503 (2008).
- [14] X. Moya, L. E. Hueso, F. Maccherozzi, A. I. Tovstolytkin, D. I. Podyalovskii, C. Ducati, L. C. Phillips, M. Ghidini, O. Hovorka, A. Berger, M. E. Vickers, E. Defay, S. S. Dhesi, and N. D. Mathur, "Giant and reversible extrinsic magnetocaloric effects in $\text{La}_{0.7}\text{Ca}_{0.3}\text{MnO}_3$ films due to strain," *Nat. Mater.* **12**, 52–58 (2013).
- [15] V. Sokolovskiy, V. Buchelnikov, M. Zagrebin, P. Entel, S. Sahoo, and M. Ogura, "First-principles investigation of chemical and structural disorder in magnetic $\text{Ni}_2\text{Mn}_{1+x}\text{Sn}_{1-x}$ heusler alloys," *Phys. Rev. B* **86**, 134418 (2012).
- [16] A. Fujita, D. Matsunami, and H. Yako, "Realization of small intrinsic hysteresis with large magnetic entropy change in $\text{La}_{0.8}\text{Pr}_{0.2}(\text{Fe}_{0.88}\text{Si}_{0.10}\text{Al}_{0.02})_{13}$ by controlling itinerant-electron characteristics," *Appl. Phys. Lett.* **104**, 122410 (2014).
- [17] Julia Lyubina, "Recent advances in the microstructure design of materials for near room temperature magnetic cooling," *J. Appl. Phys.* **109**, 07A902 (2011).
- [18] R. Niemann, S. Hahn, A. Diestel, A. Backen, L. Schultz, K. Nielsch, M. F.-X. Wagner, and S. Fähler, "Reducing the nucleation barrier in magnetocaloric heusler alloys by nanoindentation," *APL Mater.* **4**, 064101 (2016).
- [19] N. Menyuk, J.A. Kafalas, K. Dwight, and J.B. Goodenough, "Effects of pressure on the magnetic properties of MnAs," *Phys. Rev.* **177**, 942 (1969).
- [20] M. Trassinelli, M. Marangolo, M. Eddrief, V. H. Etgens, V. Gafton, S. Hidki, E. Lacaze, E. Lamour, C. Prigent, J.-P. Rozet, S. Steydli, Y. Zheng, and D. Vernhet, "Suppression of the thermal hysteresis in magnetocaloric MnAs thin film by highly charged ion bombardment," *Appl. Phys. Lett.* **104**, 081906 (2014).
- [21] M. Trassinelli, L. Bernard Carlsson, S. Cervera, M. Eddrief, V. H. Etgens, E. V. Gafton, E. Lacaze, E. Lamour, A. Lévy, S. Macé, C. Prigent, J. P. Rozet, S. Steydli, M. Marangolo, and D. Vernhet, "Low energy ne ion beam induced-modifications of magnetic properties in MnAs thin films," *J. Phys. Condens. Matter* **29**, 055001 (2017).
- [22] R. Breitwieser, Franck Vidal, I.L. Graff, Massimiliano Marangolo, Mahmoud Eddrief, J.-C. Boulliard, and VH Etgens, "Phase transition and surface morphology of MnAs/GaAs (001) studied with in situ variable-temperature scanning tunneling microscopy," *Phys. Rev. B* **80**, 045403 (2009).
- [23] L. Däweritz, "Interplay of stress and magnetic properties in epitaxial MnAs films," *Rep. Prog. Phys.* **69**, 2581 (2006).
- [24] R.H. Wilson and J.S. Kasper, "The crystal structure of mnas above 40 c," *Acta Crystallogr.* **17**, 95–101 (1964).
- [25] A. Gumberidze, M. Trassinelli, N. Adrouche, C. I. Szabo, P. Indelicato, F. Haranger, J. M. Isac, E. Lamour, E. O. Le Bigot, J. Merot, C. Prigent, J. P. Rozet, and D. Vernhet, "Electronic temperatures, densities, and plasma X-ray emission of a 14.5 GHz electron-cyclotron resonance ion source," *Rev. Sci. Instrum.* **81**, 033303–10 (2010).
- [26] M. Nastasi, J. Mayer, and J.K. Hirvonen, *Ion-Solid Interactions: Fundamentals and Applications* (Cambridge University Press, 1996).
- [27] Kai Nordlund, Steven J. Zinkle, Andrea E. Sand,

- Fredric Granberg, Robert S. Averback, Roger E. Stoller, Tomoaki Suzudo, Lorenzo Malerba, Florian Banhart, William J. Weber, Francois Willaime, Sergei L. Dudarev, and David Simeone, “Primary radiation damage: A review of current understanding and models,” *J. Nucl. Mater* **512**, 450–479 (2018).
- [28] K. Nordlund, “Historical review of computer simulation of radiation effects in materials,” *J. Nucl. Mater* **520**, 273–295 (2019).
- [29] Milan Bratko, Kelly Morrison, Ariana de Campos, Sergio Gama, Lesley F. Cohen, and Karl G. Sandeman, “History dependence of directly observed magnetocaloric effects in (Mn,Fe)As,” *Appl. Phys. Lett.* **100**, 252409 (2012).
- [30] Giorgio Bertotti, “Physical interpretation of eddy current losses in ferromagnetic materials. i. theoretical considerations,” *J. Appl. Phys.* **57**, 2110–2117 (1985).
- [31] Giorgio Bertotti, *Hysteresis in Magnetism: for Physicists, Materials Scientists, and Engineers* (Academic Press, 1998).
- [32] F. Vidal, O. Pluchery, N. Witkowski, V. Garcia, M. Marangolo, V. H. Etgens, and Y. Borenstein, “ $\alpha - \beta$ phase transition in MnAs/GaAs (001) thin films: An optical spectroscopic investigation,” *Phys. Rev. B* **74**, 115330 (2006).
- [33] V.M. Kaganer, B. Jenichen, F. Schippan, W. Braun, L. Däweritz, and K.H. Ploog, “Strain-mediated phase coexistence in heteroepitaxial films,” *Phys. Rev. Lett.* **85**, 341 (2000).
- [34] V.M. Kaganer, B. Jenichen, F. Schippan, W. Braun, L. Däweritz, and K.H. Ploog, “Strain-mediated phase coexistence in MnAs heteroepitaxial films on GaAs: An x-ray diffraction study,” *Phys. Rev. B* **66**, 045305 (2002).
- [35] T. Plake, M. Ramsteiner, V.M. Kaganer, B. Jenichen, M. Kästner, L. Däweritz, and K.H. Ploog, “Periodic elastic domains of coexisting phases in epitaxial MnAs films on GaAs,” *Appl. Phys. Lett.* **80**, 2523–2525 (2002).
- [36] T. Plake, T. Hesjedal, J. Mohanty, M. Kästner, L. Däweritz, and K.H. Ploog, “Temperature-dependent magnetic force microscopy investigation of epitaxial MnAs films on GaAs (001),” *Appl. Phys. Lett.* **82**, 2308–2310 (2003).
- [37] L. Däweritz, M. Kästner, T. Hesjedal, T. Plake, B. Jenichen, and K.H. Ploog, “Structural and magnetic order in MnAs films grown by molecular beam epitaxy on GaAs for spin injection,” *Cryst. Growth* **251**, 297–302 (2003).
- [38] James F. Ziegler and Jochen P. Biersack, “The stopping and range of ions in matter,” in *Treatise on Heavy-Ion Science: Volume 6: Astrophysics, Chemistry, and Condensed Matter*, edited by D. Allan Bromley (Springer US, Boston, MA, 1985) pp. 93–129.
- [39] James F. Ziegler, M. D. Ziegler, and J. P. Biersack, “SRIM - the stopping and range of ions in matter (2010),” *Nucl. Instrum. Methods B* **268**, 1818–1823 (2010).
- [40] R. E. Stoller, M. B. Toloczko, G. S. Was, A. G. Certain, S. Dwaraknath, and F. A. Garner, “On the use of srim for computing radiation damage exposure,” *Nucl. Instrum. Methods B* **310**, 75–80 (2013).
- [41] K. Nordlund, J. Keinonen, M. Ghaly, and R. S. Averback, “Coherent displacement of atoms during ion irradiation,” *Nature* **398**, 49–51 (1999).
- [42] A. F. Calder, D. J. Bacon, A. V. Barashev, and Yu N. Osetsky, “On the origin of large interstitial clusters in displacement cascades,” *Philos. Mag.* **90**, 863–884 (2010).
- [43] Sang-Pil Kim, Huck Beng Chew, Eric Chason, Vivek B. Shenoy, and Kyung-Suk Kim, “Nanoscale mechanisms of surface stress and morphology evolution in fcc metals under noble-gas ion bombardments,” *Proc. R. Soc. A* **468**, 2550–2573 (2012).
- [44] Chenyang Lu, Ke Jin, Laurent K. Béland, Feifei Zhang, Taini Yang, Liang Qiao, Yanwen Zhang, Hongbin Bei, Hans M. Christen, Roger E. Stoller, and Lumin Wang, “Direct observation of defect range and evolution in ion-irradiated single crystalline Ni and Ni binary alloys,” *Sci. Rep.* **6**, 19994 (2016).
- [45] V. Uhlíř, Jon Ander Arregi, and Eric E. Fullerton, “Colossal magnetic phase transition asymmetry in mesoscale ferri stripes,” *Nat. Commun.* **7** (2016).
- [46] Lev Davidovich Landau, Evgenij M Lifšic, Evgenii Mikhailovich Lifshitz, Arnold Markovich Kosevich, and Lev Petrovich Pitaevskii, *Theory of elasticity: volume 7*, Vol. 7 (pergamon, Oxford, 1986).
- [47] Frank Reginald Nunes Nabarro, “Mathematical theory of stationary dislocations,” *Adv. Phys.* **1**, 269–394 (1952).
- [48] Maurice Klemen and Oleg D. Lavrentovich, *Soft matter physics: an introduction* (Springer, 2003).
- [49] Johannes W. van der Jagt, Vincent Jeudy, André Thiaville, Mamour Sall, Nicolas Vernier, Liza Herrera Diez, Mohamed Belmeguenai, Yves Roussigné, Salim M Chérif, Mouad Fattouhi, *et al.*, “Revealing nanoscale disorder in W/Co-Fe-B/MgO ultrathin films using domain-wall motion,” *Phys. Rev. Appl.* **18**, 054072 (2022).